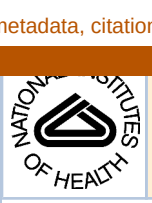

Published in final edited form as:

Chem Commun (Camb). 2010 June 21; 46(23): 4139–4141. doi:10.1039/c0cc00179a.

Manganese displacement from Zinpyr-1 allows zinc detection by fluorescence microscopy and magnetic resonance imaging†

Youngmin You[a,b], **Elisa Tomat**[a], **Kevin Hwang**[a], **Tatjana Atanasijevic**[c], **Wonwoo Nam**[b], **Alan P. Jasanoff**[c], and **Stephen J. Lippard**[a,*]

[a]Department of Chemistry, Massachusetts Institute of Technology, Cambridge, Massachusetts 02139

[b]Department of Chemistry and Nano Science and Department of Bioinspired Science, Ewha Womans University, Seoul 120–750 Korea

[c]Department of Biological Engineering, Massachusetts Institute of Technology

Abstract

A paramagnetic manganese complex of a fluorescein-based probe affords a dual-modality zinc sensor featuring an improved fluorescence dynamic range and an MRI readout.

Several metal-based receptors have been employed in displacement assays1 to detect biologically relevant analytes, such as carbonate,2 phosphate,3 and nitric oxide.4 In optical sensors that provide a fluorescence readout, the emissive reporter is typically quenched by coordination of a paramagnetic metal ion, which is displaced by the analyte to provide an increase in emission intensity. Alternatively, fluorescent detection systems can exploit differences in binding affinities of two coordinating cations and in the optical properties of their corresponding complexes. For instance, transmetalation reactions involving Zn(II) and Cd(II) convey ratiometric sensing of these ions in neutral aqueous solutions.5, 6 In addition, Hg(II) ions liberate Cu(II) from a fluorescent receptor to give emission turn-on in DMSO/water solution.7 Recently, we demonstrated that displacement of Mn(II) from polydentate chelating agents allows Ca(II) detection by magnetic resonance imaging (MRI) in vitro.8 In the present report, we recapitulate the design of displacement probes in a dual-modality Mn(II)-based system that allows zinc detection by both fluorescence and MRI readouts.

The development of fluorescent sensors featuring a wide dynamic range (Φ_{metal}/Φ_{free}) is one of the current challenges in the field of biological zinc detection.9, 10 We reasoned that background fluorescence derived from fluorophores in the zinc-free state, including proton-induced fluorescence, could be avoided by pre-complexation of the sensor with a paramagnetic ion, which can quench sensor fluorescence by acting as the acceptor in a nonradiative energy- or electrontransfer process. Displacement of the paramagnetic center by zinc coordination would then afford a highly emissive zinc complex and hence a turn-on signal. For intracellular imaging, use of Mn(II) as the paramagnetic center is preferrable when compared to other ions employed in displacement assays, such as toxic Cd(II)6 and tightly regulated Cu(II).7 A Mn(II) displacement approach is employed herein to improve the fluorescence dynamic range of Zinpyr-1 (ZP1, Scheme 1), a zinc-responsive fluorescent indicator that has found wide applicability for the detection of biological mobile zinc.[11, 12]

†Electronic supplementary information (ESI) available: Experimental details, fluorescence titrations, fluorescence cell images and MRI data. See http://dx.doi.org/10.1039/b000000x/

Fax: +1-617-253-1892; Tel:+1-617-258-8150; lippard@mit.edu.

The fluorescence intensity of ZP1 decreases ($\Phi_{free} = 0.17 \rightarrow \Phi_{Mn} = 0.0067$) promptly upon addition of $MnCl_2$, leveling off after 2 equiv. The stoichiometry for the ZP1–Mn^{2+} complex ([$ZP1Mn_2$]) is 1:2 as revealed by a fluorescence Job's plot and a mole ratio plot (ESI†). Apparent dissociation constant values for the [$ZP1Mn_2$] complex were obtained by non-linear least-square fitting of fluorescence titration data to give 0.55 μM and 2.2 μM for the first and second binding events, respectively. These K_d values are ca. 10^{10} and 10^3 times greater than those for Zn(II) in [$ZP1Zn_2$],[13] indicating that manganese displacement by zinc ions is thermodynamically highly favored. As expected, addition of $ZnCl_2$ to a [$ZP1Mn_2$] solution immediately enhanced fluorescence emission (Fig. 1) due to formation of [$ZP1Zn_2$] (Φ_{Zn} = 0.71). The Zn(II)-induced fluorescence response for the displacement reaction was as fast as that of simple Zn(II) association in the time scale of our steady-state measurements (i.e., typically 1 titrant addition per minute). The corresponding fluorescence dynamic range increases by 25-fold, from 4 for ZP1 to 106 for [$ZP1Mn_2$]. This improved fluorescence turn-on persists even in the presence of a large excess of Mn^{2+} (up to 1000 equiv, ESI†). Although the fluorescence dynamic range decreases at pH 6.0 and 8.0, it remains at a relatively high level (31 and 36, respectively) (Fig. 1). In addition, [$ZP1Mn_2$] selects Zn^{2+} over biologically abundant metal ions such as Na^+, K^+, Ca^{2+} and Mg^{2+}. Hg^{2+} and Cd^{2+} ions displace Mn^{2+} to enhance fluorescence, which further increases after addition of Zn^{2+}. In contrast, as expected from the Irving–Williams series, Zn^{2+}-induced fluorescence turn-on does not occur in the presence of the tightly binding paramagnetic Cu^{2+}, Co^{2+} and Fe^{2+} ions.

The [$ZP1Mn_2$] probe was employed to detect exogenous zinc in live cell imaging experiments. HeLa cells were incubated with [$ZP1Mn_2$] (10 μM), which proved to be cell-permeable and non-toxic. For direct comparison, cells were similarly treated with unmetallated ZP1. As shown in Fig. 2, almost no background signal is observed for [$ZP1Mn_2$]-treated HeLa cells, whereas broad fluorescent halos appear in ZP1-treated cells. Exogenously supplied Zn^{2+} ($ZnCl_2$/sodium pyrithione, 1:1, 50 μM) causes the appearance of bright signals. Although the physiological effects of liberated Mn^{2+} ions were not investigated in detail, the overall morphology of cells appeared intact after displacement. Compared to ZP1, [$ZP1Mn_2$] affords superior fluorescence contrast, a definite benefit of the reduced background emission. Additional incubation with *N*,*N*,*N*′,*N*′-tetra(2-picolyl)ethylenediamine (TPEN, 50 μM) reduced the fluorescence signal, as expected for a zinc-responsive turn-on probe (ESI†).

The displacement of paramagnetic Mn^{2+} ions (S = 5/2) offers the potential for metal-responsive MRI readout derived from the concurrent change in magnetic relaxation of inner/outer-sphere water molecules. This type of MRI signal generation relies on changes in the number (*q*) of sites available for water coordination to the manganese center before and after zinc-induced displacement. This approach was recently examined in our laboratories for the detection of Ca^{2+} ion.[8] Moreover, the transmetalation of a manganese complex with zinc ions is reminiscent of the pharmacokinetics of Teslascan™,[14, 15] a clinically approved MRI contrast agent containing manganese *N*,*N*′-dipyridoxylethylenediamine-*N*,*N*′-diacetate-5,5'-bis(phosphate) as the active ingredient. The foregoing reports prompted us to consider [$ZP1Mn_2$] as a potential zinc-responsive MRI contrast agent.

For MRI experiments, the central 16 wells of microtiter plates were filled with various samples prepared in buffered aqueous solutions (see ESI for details†). Complexation of Mn^{2+} ion enhances the water-solubility of the complex, a desirable feature for MRI experiments. As shown in Fig. 3, [$ZP1Mn_2$] is zinc-responsive under MRI observation, with T_2 decreasing after addition of Zn^{2+}. The corresponding transverse relaxivity (r_2) change is ca. 1.7-fold, from 41 (±1) mM^{-1} s^{-1} to 67 (±0) mM^{-1} s^{-1} and from 40 (±3) mM^{-1} s^{-1} to 68 (±4) mM^{-1} s^{-1} for

†Electronic supplementary information (ESI) available: Experimental details, fluorescence titrations, fluorescence cell images and MRI data. See http://dx.doi.org/10.1039/b000000x/

perchlorate- and chloride-containing buffer, respectively. These changes are consistent with an increase in q following Mn^{2+} ion displacement, in agreement with the fluorescence results. Control experiments and relaxivity measurements as a function of zinc concentration unambiguously indicate that [ZP1Mn_2] responds to Zn^{2+} in the micromolar range (ESI†). The smaller Δr_2 values compared to those observed for our previous systems based on hexadentate chelators (i.e., ethylene glycol-bis(2-aminoethylether)-*N*,*N*,*N*′,*N*′-tetraacetic acid (EGTA), 1,2-bis(2-aminophenoxy)ethane-*N*,*N*,*N*′,*N*′-tetraacetic acid (BAPTA))[8] are most likely a consequence of water coordination ($q > 0$) to the Mn^{2+} center in [ZP1Mn_2] prior to zinc addition. Changes in longitudinal relaxivity (r_1) computed from T_1-weighted MRI signals were within the error of the measurements and hence did not allow estimation of a zinc-induced response.

To summarize, a paramagnetic Mn^{2+}–fluorophore complex was able to serve as a dual probe for zinc. Mn^{2+} displacement by Zn^{2+} ions in ZP1 results in an improved fluorescence dynamic range, both in the cuvette and in live cells. In addition, the successful demonstration of MRI using [ZP1Mn_2] suggests a route to dual-modality imaging[16] based on paramagnetic displacement strategies. Notably, this dual-mode detection requires neither additional modifications[17] nor integration of discrete functionalities[18] for fluorescence and MRI readout, because the identical chemical event (Mn^{2+} displacement) triggers both signal outputs. Although the release of paramagnetic ions is not suitable for all experimental settings, such sensing mechanisms could provide versatile tools to the vibrant field of zinc bioimaging[9, 10] by allowing description of zinc trafficking at both the cellular and organismal levels.

Supplementary Material

Refer to Web version on PubMed Central for supplementary material.

Acknowledgments

This work was supported by a grant from the National Institute of General Medical Sciences (Grant GM065519 to SJL). Spectroscopic instrumentation at the MIT DCIF is maintained with funding from NIH Grant 1S10RR13886-01. YY and WN are grateful for financial assistance from RP-Grant 2010 of Ewha Womans University and SBS Foundation, Seoul, Korea to support their postdoctoral and sabbatical stays at MIT, respectively. TA and APJ acknowledge support from NIH Grant DP2-OD2441 and from the Raymond & Beverley Sackler Foundation.

Notes and references

1. Nguyen BT, Anslyn EV. Coord. Chem. Rev 2006;250:3118–3127.
2. Fabbrizzi L, Leone A, Taglietti A. Angew. Chem. Int. Ed 2001;40:3066–3069.
3. Tobey SL, Anslyn EV. Org. Lett 2003;5:2029–2031. [PubMed: 12790520]
4. Hilderbrand SA, Lim MH, Lippard SJ. J. Am. Chem. Soc 2004;126:4972–4978. [PubMed: 15080703]
5. Xu Z, Baek K-H, Kim HN, Cui J, Qian X, Spring DR, Shin I, Yoon J. J. Am. Chem. Soc 2010;132:601–610. [PubMed: 20000765]
6. Xue L, Liu Q, Jiang H. Org. Lett 2009;11:3454–3457. [PubMed: 19719190]
7. He G, Zhao Y, He C, Liu Y, Duan C. Inorg. Chem 2008;47:5169–5176. [PubMed: 18479122]
8. Atanasijevic T, Zhang X-a, Lippard SJ, Jasanoff A. Inorg. Chem 2010;49:2589–2591. [PubMed: 20141114]
9. Que EL, Domaille DW, Chang CJ. Chem. Rev 2008;108:1517–1549. [PubMed: 18426241]
10. Tomat E, Lippard SJ. Curr. Opin. Chem. Biol 2010;14:225–230. [PubMed: 20097117]
11. Walkup GK, Burdette SC, Lippard SJ, Tsien RY. J. Am. Chem. Soc 2000;122:5644–5645.
12. Ketterman JK, Li YV. J. Neurosci. Res 2007;86:422–434. [PubMed: 17847078]
13. Wong BA, Friedle S, Lippard SJ. J. Am. Chem. Soc 2009;131:7142–7152. [PubMed: 19405465]

14. Toft KG, Hustvedt SO, Grant D, Gordon PB, Friisk GA, Korsmo AJ, Skotland T. Acta Radiol 1997;38:677–689. [PubMed: 9245963]
15. Schmidt PP, Toft KG, Skotland T, Andersson KK. J. Biol. Inorg. Chem 2002;7:241–248. [PubMed: 11935348]
16. Jennings LE, Long NJ. Chem. Commun 2009:3511–3524.
17. Zhang, X-a; Lovejoy, KS.; Jasanoff, A.; Lippard, SJ. Proc. Natl. Acad. Sci. USA 2007;104:10780–10785. [PubMed: 17578918]
18. Lee J-H, Jun Y-w, Yeon S-I, Shin J-S, Cheon J. Angew. Chem. Int. Ed 2006;45:8160–8162.

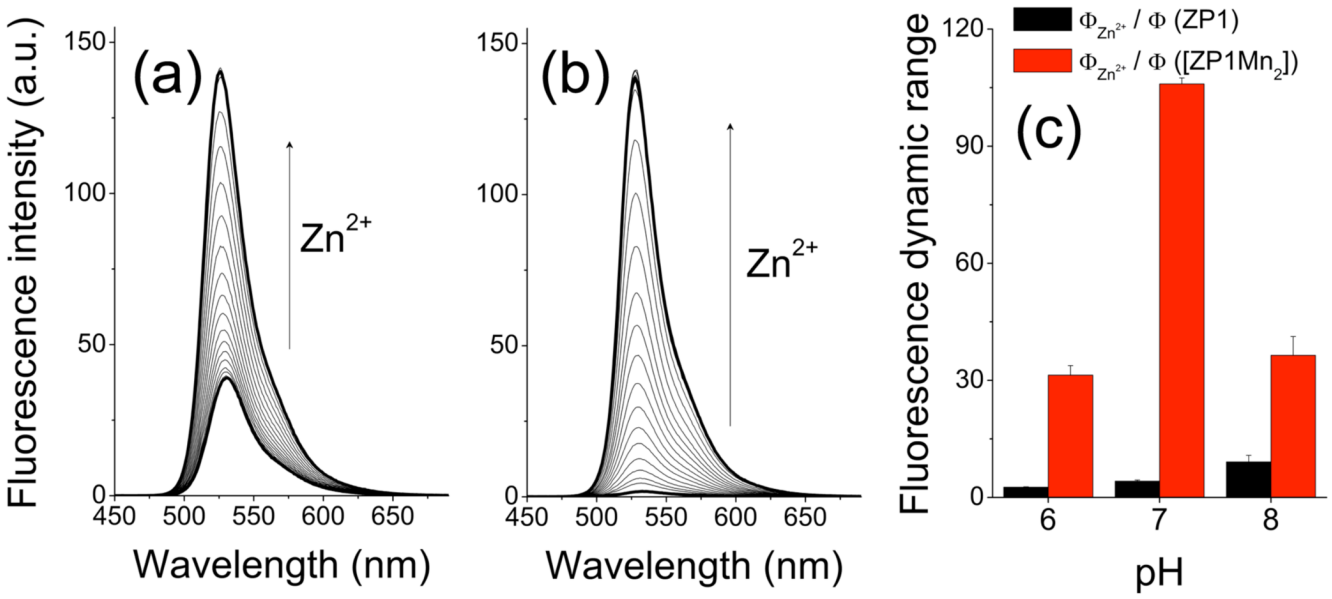

Fig. 1.

Zinc-induced (0 to 3 equiv) fluorescence enhancement of (a) ZP1 and (b) [ZP1Mn_2] at pH 7.0 (10 μM). (c) Fluorescence dynamic range (Φ_{Zn}/Φ_{free}) of ZP1 (black) and [ZP1Mn_2] (red) at pH 6.0 (50 mM MES, 100 mM KCl), 7.0 (50 mM PIPES, 100 mM KCl) and 8.0 (25 mM HEPES, 100 mM KCl).

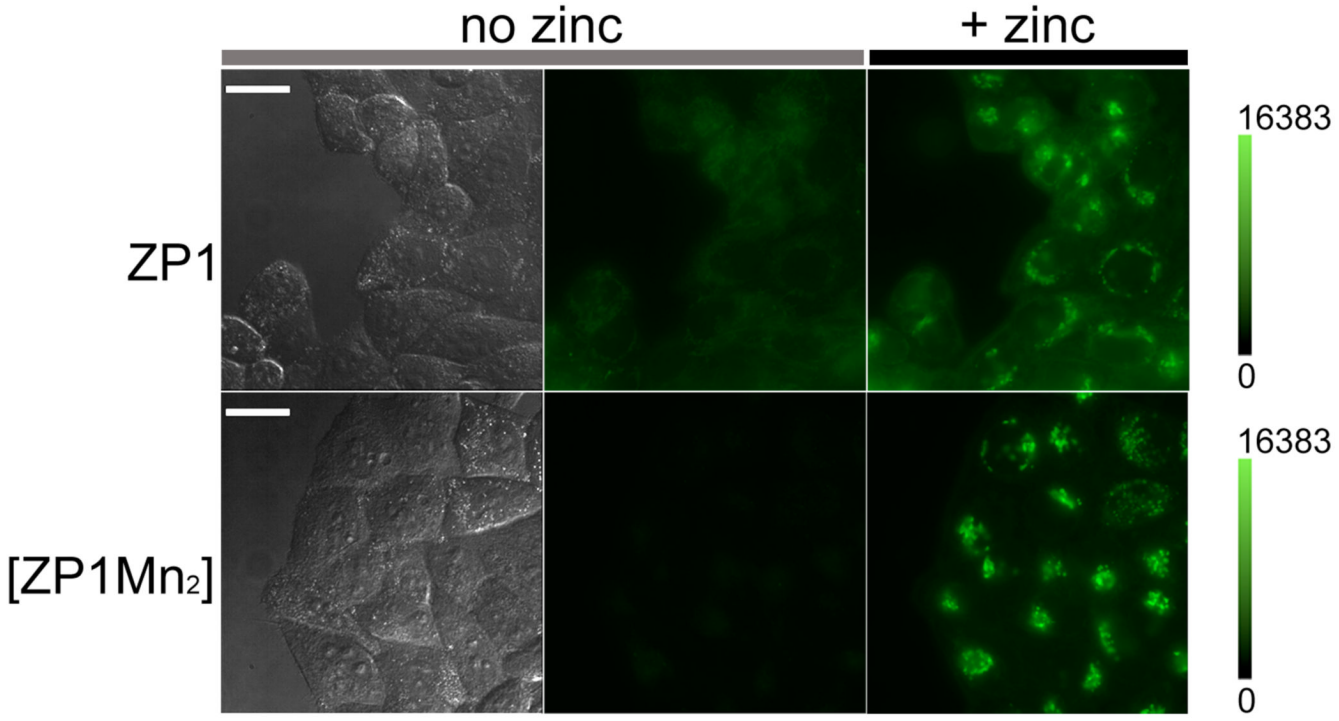

Fig. 2.

Fluorescence microscopy images of HeLa cells incubated with ZP1 or [$ZP1Mn_2$]. Left: DIC images (scale bar = 25 μm), middle: background fluorescence images, right: zinc-induced response fluorescence images. Micrographs are shown relative to the same intensity scale for direct comparison.

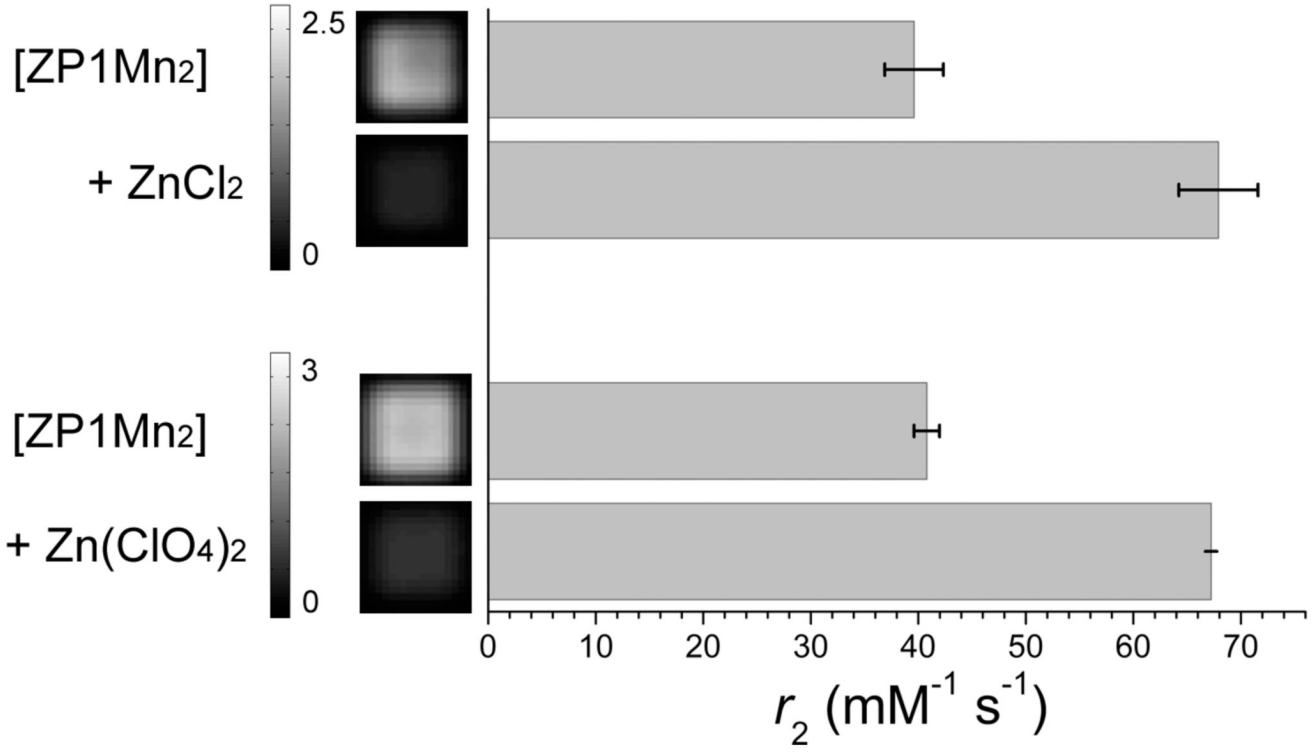

Fig. 3.

T_2-weighted MRI (TR = 2000 ms, TE = 80 ms, field strength = 200 MHz. Scale bars represent acquired MRI signal intensity (/10^5)) and transverse relaxivity (r_2) of [ZP1Mn$_2$] (0.1 mM) before and after addition of $ZnCl_2$ or $Zn(ClO_4)_2$ (2 mM) in 50 mM PIPES buffer containing either KCl or $KClO_4$ (100 mM), respectively, pH 7.0.

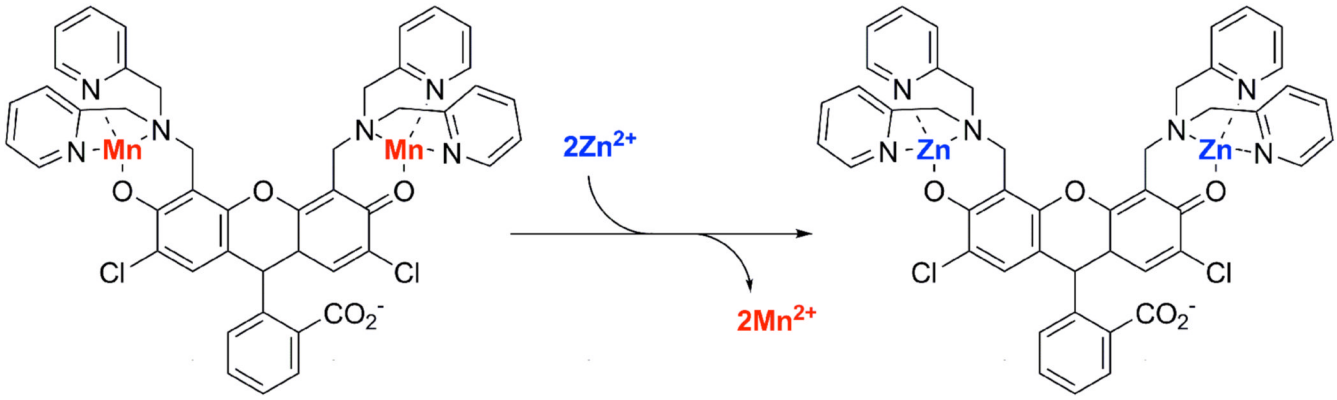

Scheme 1.
Complex [ZP1Mn_2] and displacement reaction